

## Low temperature properties of pnictide CrAs single crystal

WU Wei, ZHANG XiaoDong, YIN ZhiHua, ZHENG Ping, WANG NanLin & LUO JianLin\*

*Beijing National Laboratory for Condensed Matter Physics, Institute of Physics, Chinese Academy of Sciences, Beijing 100190, China*

Received April 16, 2010; accepted May 16, 2010

High quality single crystal CrAs was grown by Sn flux method. The results of magnetic susceptibility and electrical resistivity are reported in a temperature range of 2 to 800 K. At low temperatures, a  $T^2$  dependence of resistivity is observed showing a Fermi-liquid behavior. The Kadowaki-Woods ratio is found to be  $1 \times 10^{-5} \mu\Omega \text{ cm mol}^2 \text{ K}^2 \text{ mJ}^{-2}$ , which fits well to the universal value for many correlated electron systems. At about 270 K, a clear magnetic transition is observed with sharp changes of resistivity and susceptibility. Above 270 K, a linear-temperature dependence of the magnetic susceptibility is observed up to 700 K, which resembles the  $T$ -dependent magnetic susceptibility of parents of iron-pnictides superconductors.

**CrAs, Kadowaki-Woods ratio, magnetic phase transition, linear  $T$ -dependent magnetic susceptibility**

**PACS:** 74.70.-b, 74.62.Bf, 74.25.Gz

### 1 Introduction

Since the discovery of superconductivity in the newly discovered rare-earth iron-based oxide systems, much efforts have been made to explore similar phenomena in other transition metal oxides and pnictides. Up to date, several different crystal structures of iron pnictides (or chalcogenides) were discovered and found to exhibit high  $T_c$  superconductivity by either doping or application of pressure [1–5], including LnFeAsO (Ln = rare earth, so called 1111 system), AFe<sub>2</sub>As<sub>2</sub> (A = Ca, Sr, Ba, 122), LiFeAs(111), and FeSe<sub>1- $\delta$</sub> (11) [6–9]. All these iron-pnictide superconductors have a layered structure with two-dimensional FePn (Pn = pnictogen/chalcogen) conducting layers. Except for a relatively high transition temperature, the systems display interesting magnetic properties. The FeAs-based parent compounds commonly show collinear antiferromagnetic type spin-density-wave (SDW) ordering. The superconductivity is found to be in the vicinity of the SDW. In addition, the recent inelastic neutron scattering experiments showed the

presence of the incommensurate magnetic resonance peak near the wave vector  $Q = (0.5, 0.5, 0)$  in superconducting states of (BaK)Fe<sub>2</sub>As<sub>2</sub> and FeSe superconductors, similar to that of the high  $T_c$  cuprates. These observations reveal that the magnetism plays a crucial role in driving the superconductivity in those materials [10–15].

CrAs is one of the intermetallic pnictides with crystal structure of orthorhombic MnP-type as shown in Figure 1(a). The lattice parameters are  $a=5.649 \text{ \AA}$ ,  $b=3.463 \text{ \AA}$ , and  $c = 6.2084 \text{ \AA}$  [16]. The structural, magnetic, specific heat, transport, and neutron scattering measurements have been reported for polycrystal materials [16–19]. The compound has a phase transition at 800 K from the hexagonal NiAs-type to the orthorhombic MnP-type. Similar to parent of iron pnictides superconductors, the neutron scattering experiments reveal that below 270 K, CrAs is magnetically ordered and the magnetic structure of which is a double-helical one propagating along the  $b$ -axis [17]. The spin orientation in the helimagnetic structure of CrAs is shown in Figure 1(b). All magnetic moments lie essentially in  $a$ - $c$  plane, and it is seen that the spins on atoms 2 and 3 are almost antiparallel arranged. The spins on atom 1 and 2 show

\*Corresponding author (email: JLLuo@aphy.iphy.ac.cn)

a noncollinear arrangement. A first-order transition accompanying the abrupt changes of lattice parameters occurs at transition temperature ( $T_N$ ). However, it is surprised that no any remarkable anomaly in resistivity and magnetic susceptibility around 270 K for polycrystalline samples. So, it would be interesting to study the properties of high quality single crystal CrAs and compare results with that of iron-pnictide superconductors.

In this paper, we report resistivity (2–300 K) and magnetic susceptibility (2–800 K) results obtained with high quality CrAs single crystals. A clear magnetic phase transition is observed at 270 K in both resistivity and susceptibility measurements. In addition, we found that at low temperatures, the resistivity shows a  $T^2$  dependence indicating a Fermi-liquid ground state. The Kadowaki-Woods ratio is found to be  $1 \times 10^{-5} \mu\Omega \text{ cm mol}^2 \text{ K}^2 \text{ mJ}^{-2}$ , which is a universal value for correlated electron systems. Above magnetic transition temperature, a linear-temperature dependence of the magnetic susceptibility is observed up to 700 K, which resembles the  $T$ -dependent magnetic susceptibility of parents of the iron-pnictide superconductors, such as LaOFeAs, BaFe<sub>2</sub>As<sub>2</sub>, and CaFe<sub>2</sub>As<sub>2</sub> [20–23].

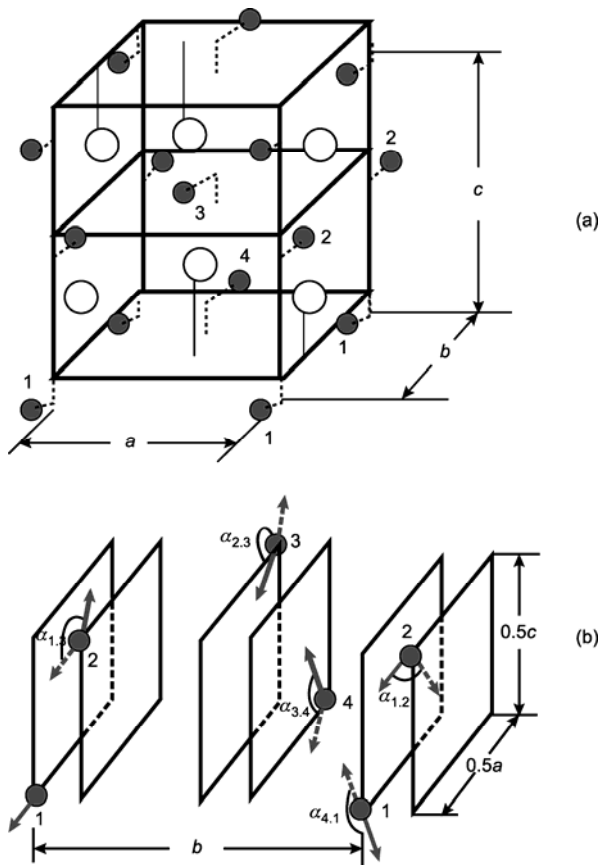


**Figure 1** Lattice structure and spin structure of CrAs. (a) The unit cells of the orthorhombic MnP-type (low temperature phase below 800 K) crystal,  $\bullet$  and  $\circ$  denote the Cr and As atoms, respectively; (b) double helical spin structure of CrAs, where only the metallic atom sites 1, 2, 3, and 4 are shown. The angles  $\alpha_{1,2} = \alpha_{3,4} = -120^\circ$ , and  $\alpha_{2,3} = \alpha_{3,4} = 185^\circ$ .

## 2 Experiments

The CrAs crystals were grown using Sn-flux method. The starting materials were Cr (Cerac, powder, 99.9%), As (Alfa Aesar, powder, 99.99%), and Sn (Cerac, shot, 99.9%). All of the manipulations were done in an Argon-filled glove box with moisture and oxygen levels less than 1 ppm. The materials with atomic ratio of Cr:As:Sn = 3:4:40 were added to an alumina crucible, which was placed in a quartz ampoule, and subsequently sealed under a reduced pressure of  $10^{-4}$  Torr. The quartz ampoule was heated up to  $650^\circ\text{C}$  for 10 h, held there for a period of 8 h, then heated up to  $1000^\circ\text{C}$  for 15 h, held for 6 h, and slowly cooled down to  $600^\circ\text{C}$  for 50 h. At this temperature, liquid Sn flux was filtered by centrifugation. The resulting products were metallic needle-shaped black crystals with dimensions up to  $0.15 \times 0.15 \times 1 \text{ mm}^3$ . The crystals were grown along the  $b$ -axis and they are stable in air and water.

Energy-dispersive X-ray (EDX) analysis on these crystals was carried out using a Hitachi S-2700 scanning electron microscope. The results show that the chemical compositions are 51(2)% Cr, and 49(2)% As. No Sn elements were detected in the crystals analyzed. The magnetic susceptibility was measured in temperature range of 2–300 K using a SQUID VSM Magnetometer of Quantum Design Company, and in temperature range of 300–800 K using a VSM Magnetometer installed in PPMS system of Quantum Design Company. The resistivity was measured between 2 and 300 K by the standard 4-probe method. The current was applied along the  $b$ -axis of the crystal.

## 3 Results and discussion

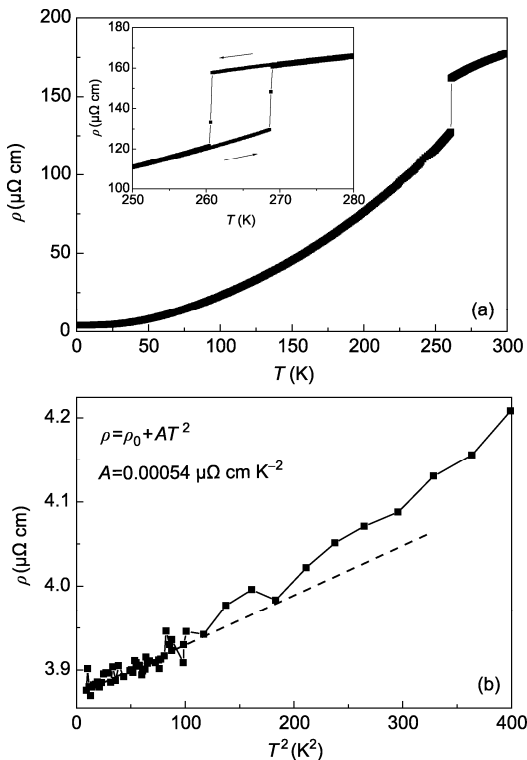
### 3.1 Resistivity

Figure 2(a) shows the resistivity ( $\rho$ ) as a function of temperature between 2 and 300 K. The  $\rho(T)$  shows a typical metallic behavior over the measured temperature range 2–300 K. The residual resistivity is  $3.87 \mu\Omega \text{ cm}$ . The residual resistivity ratio (RRR):  $\rho(300 \text{ K})/\rho(4.2 \text{ K}) = 50$ , much larger than that of the single crystal of parents of iron-pnictides (usually less than 10), suggests a high quality of the crystal compared with that of the iron-pnictides. A sharp decrease in the electrical resistivity at  $T_N = 270 \text{ K}$  is observed. This indicates that the spin-disorder scattering is significantly reduced in the magnetic ordered metallic state below  $T_N$ . A large thermal hysteresis of about 10 K is observed around 270 K for the resistivity measurement (see inset of Figure 1(a)), evidencing a first-order phase transition. Such a result is consistent with the experimental result that the magnetic transition is accompanying with a structural transition as reported by Kanaya et al. [17,18]. The lattice parameter  $b$  increases abruptly by 4%, while the  $a$  and  $c$  decrease by less than 1% below 270 K. Our result is different

from the pervious work where the resistivity of CrAs increases with decreasing temperature below 270 K [16]. The behavior that the magnetic transition occurs concomitantly with a structural distortion is similar to that of 122 systems of iron-pnictides. In the 122 systems such as SrFe<sub>2</sub>As<sub>2</sub>, the antiferromagnetic ordered SDW transition occurs simultaneously with a lattice distortion from a tetragonal phase to an orthorhombic phase at the same temperature. However, for 1111 systems like the LaFeAsO, the magnetic transition is about 10 K below the structural transition.

Figure 2(b) shows resistivity versus  $T^2$ . Below 15 K, the resistivity can be well described by a constant term plus a  $T^2$  term:  $\rho(T) = \rho_0 + AT^2$ , where  $\rho_0$  is the residual resistivity and  $A$  is a constant. The existence of  $T^2$  term at low temperatures indicates Fermi-liquid ground states for CrAs. From the obtained value of  $A$ , we can readily calculate the Kadowaki-Woods ratio  $A/\gamma^2$  (where  $\gamma = 9.1$  mJ/mol K<sup>2</sup> is electronic specific heat coefficient, obtained from ref. [19]) and obtain  $a_0 = 1 \times 10^{-5} \mu\Omega \text{ cm mol}^2 \text{ K}^2 \text{ mJ}^{-2}$ . Figure 3 compares the Kadowaki-Woods ratio of CrAs with other materials. It is interesting that the Kadowaki-Woods ratio of CrAs locates on the universal line of the correlated electron systems, which is about one order larger than those of simple metals, like Fe, Ni, Cu, etc.

Various mechanisms have been proposed to explain the different Kadowaki-Woods ratios for different materials. It depends on the effects of anisotropy, carrier concentration,



**Figure 2** (a) Temperature dependence of  $b$ -axis resistivity for CrAs, the transition at 270 K can be clearly seen. The inset shows the resistivity curve of the thermal hysteresis at 270 K; (b)  $\rho$  versus  $T^2$  at low temperatures. The straight line is the fit of the low temperature part with  $\rho(T) = \rho_0 + AT^2$ .

Fermi-surface topology, magnetic correlation, ground state degeneracy, etc. For example, magnetic frustration or proximity to a quantum critical point (QCP) was considered as a reason for the large value of  $A/\gamma^2 = 60a_0$  for Na<sub>0.07</sub>CoO<sub>2</sub>; a reduced dimensionality was suggested to be the cause for enhanced Kadowaki-Woods ratio in Cu<sub>0.07</sub>TiSe<sub>2</sub> [25]. For CrAs, magnetic correlations, ground state degeneracy and a possible gap opening below the magnetic transition which depletes the DOS at Fermi level may be the cause for the increased value of  $A$  or decreased value of  $\gamma$ . Apparently, further investigations need to be carried out to understand why the Kadowaki-Woods ratio of CrAs is just on the universal line of correlated electron systems.

### 3.2 Magnetic susceptibility

Figure 4(a) shows the susceptibility  $\chi$  versus temperature between 2 and 300 K in field of  $B = 1$  T, applied both along and perpendicular to the  $b$ -axis. A linear temperature dependent susceptibility with significant anisotropy is observed above 270 K. At 270 K, contrast to the polycrystalline samples, the magnetic transition are clearly observed for both  $B//b$  and  $B\perp b$ . Similar to the resistivity measurement, a thermal hysteresis is also observed at the transition temperature, indicating the nature of first order transition.

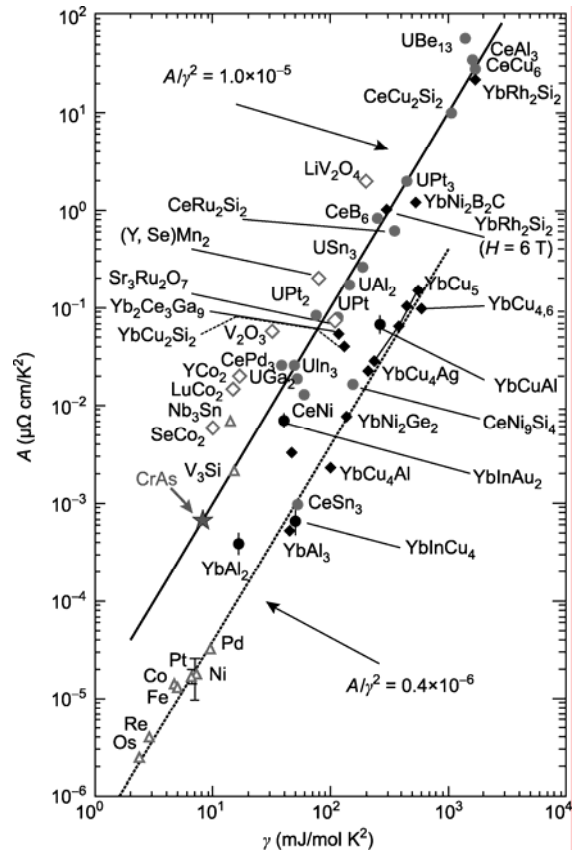


**Figure 3** Kadowaki-Woods plot ( $A$  versus  $\gamma$ ) for different materials (data obtained from ref. [23]). The position of CrAs is shown by a large star symbol.

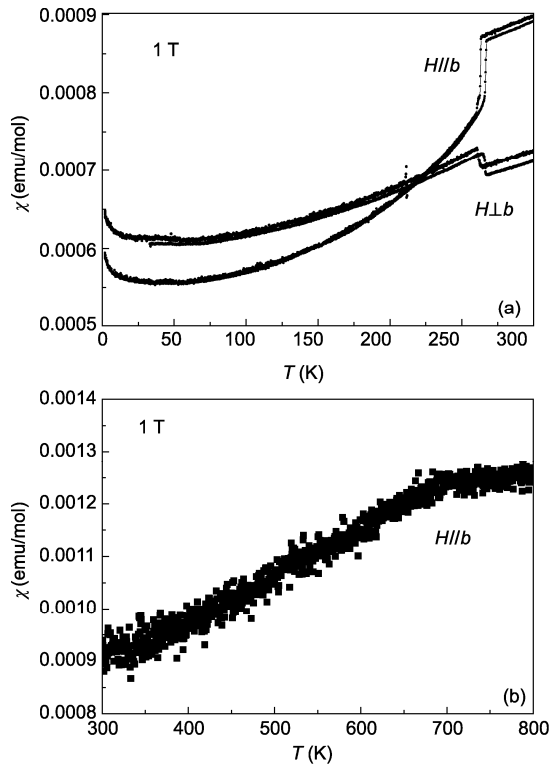


**Figure 4** (a) Magnetic susceptibility  $\chi$  versus temperature  $T$  between 2 and 300 K in the applied field of  $B = 1$  T for  $B//b$  and  $B\perp b$ , respectively; (b)  $\chi$  versus  $T$  between 300 and 800 K for  $B//b$ .

It is interesting to note that below the transition temperature,  $\chi$  behaves differently for  $B//b$  and  $B\perp b$ .  $\chi$  shows a sharp drop at first, and then decreases with decreasing  $T$  for  $B//b$ . While  $\chi$  shows a sharp jump, and then decreases with decreasing  $T$  for  $B\perp b$ . Neutron scattering experiments [17] show that the spin structure is an antiferromagnetic-type double helical structure below 270 K (see Figure 1(c)). The drop in  $\chi$  and its further decreasing with decreasing  $T$  for  $B//b$  can be understood by the presence of the antiferromagnetic fluctuations. However, it can not explain why  $\chi$  shows a sharp jump at 270 K for  $B\perp b$ . In some materials with the presence of canted-AF transition, the magnetic susceptibility shows weak ferromagnetic behavior in a certain direction.  $\chi$  increases with decreasing  $T$ . However, the  $\chi(T)$  behavior for  $B\perp b$  for CrAs can not be understood by such a canted-AF spin structure because  $\chi$  only shows a sharp jump at around 270 K but then decreases with decreasing  $T$ . We believe the different behavior in  $\chi(T)$  for  $B//b$  and  $B\perp b$  is related to structural transition. Below 270 K, the lattice parameter  $b$  increases by 4% while the  $a$  and  $c$  decreases by about 1%. Hence the spin exchange constant along  $b$ -axis,  $J_b$ , should decrease while the  $J_a$ , and  $J_c$  should increase. As a result,  $\chi(T)$  shows a sharp drop for  $B//b$  while a sharp jump  $B\perp b$  at 270 K. That the magnitude of the drop in  $\chi(T)$  for  $B//b$  is much larger than that of the jump in  $\chi(T)$  for  $B\perp b$  can be explained by the fact that the change of lat-

tice parameter  $b$  is much larger than that of  $a$  and  $c$  below 270 K.

The present susceptibility results on single crystal can also explain why susceptibility does not show any remarkable anomaly at  $T_N$  for polycrystalline in the previous work [17]. In a polycrystalline containing enormous crystals with random orientation, the susceptibility anomaly at 270 K would cancel out because of the different behavior of  $\chi(T)$  for  $B//b$  and  $B\perp b$ .

Above 270 K (Figure 4(b)),  $\chi$  increases linearly with  $T$  up to 700 K. Such a behavior is observed in iron-pnictide superconductors where the susceptibility increases linearly with  $T$  above the SDW temperature. It is also observed in other metallic materials with SDW ground state above  $T_{SDW}$  (e. g. chromium). Another prominent example is the metallic AF system  $\text{Na}_{0.5}\text{CoO}_2$  where a linear- $T$  susceptibility above  $T_N$  is observed [25]. Several different explanations to account for such linear susceptibility behavior in iron pnictides were proposed on the basis of either an itinerant picture or a local exchange picture [20]. We believe the present material with its unique spin structure may provide additional information to the understanding of the unusual linear- $T$ -dependent susceptibility in transitional metal compounds.

In addition, above 270 K, the slope of the linear magnetic susceptibility for  $B//b$  is the same as  $B\perp b$ . It may indicate that the origin of the linear-temperature dependence of magnetic susceptibility in the two orientations is essentially the same. It is interesting to note that the similar behavior also exists in many parents of iron-pnictide superconductors like  $\text{SrFe}_2\text{As}_2$  [26] and  $\text{BaFe}_2\text{As}_2$  [27].

## 4 Conclusions

We have presented investigations on the physical properties of the high quality single crystal of CrAs. At low temperatures, a  $T^2$  dependence of resistivity is observed showing a Fermi-liquid behavior. The Kadowaki-Woods ratio is found to be  $1 \times 10^{-5} \mu\Omega \text{ cm mol}^2 \text{ K}^2 \text{ mJ}^{-2}$ , locating in the universal line for many correlated electron systems. At about 270 K, a clear magnetic transition is observed with sharp changes of resistivity and susceptibility. The susceptibility displays a sharp drop for  $B//b$  but a jump for  $B\perp b$ , respectively. The behavior can be understood by the coupled magnetic and structural phase transitions that occurs simultaneously. Above 270 K, a linear-temperature dependence of the magnetic susceptibility is observed up to 700 K, which resembles the  $T$ -dependent magnetic susceptibility of parent of iron-pnictides superconductors.

*This work was supported by the National Natural Science Foundation of China, the Knowledge Innovation Project of Chinese Academy of Sciences, and the 973 Project of the MOST of China.*

- 1 Kamihara Y, Watanabe T, Hirano M, et al. Iron-based layered superconductor  $\text{La}[\text{O}_{1-x}\text{F}_x]\text{FeAs}$  ( $x = 0.05\text{--}0.12$ ) with  $T_c = 26$  K. *J Am Chem Soc*, 2008, 130: 3296–3297
- 2 Chen G F, Li Z, Wu D, et al. Superconductivity at 41 K and its competition with spin-density-wave instability in layered  $\text{CeO}_{1-x}\text{F}_x\text{FeAs}$ . *Phys Rev Lett*, 2008, 100: 247002
- 3 Chen X H, Wu T, Wu G, et al. Superconductivity at 43 K in  $\text{SmFeAsO}_{1-x}\text{F}_x$ . *Nature*, 2008, 453: 761–762
- 4 Ren Z A, Yang J, Lu W, et al. Superconductivity in the iron-based F-doped layered quaternary compound  $\text{Nd}[\text{O}_{1-x}\text{F}_x]\text{FeAs}$ . *Europhys Lett*, 2008, 82: 57002
- 5 Wang C, Li L J, Chi S, et al. Thorium-doping-induced superconductivity up to 56 K in  $\text{Gd}_{1-x}\text{Th}_x\text{FeAsO}$ . *Europhys Lett*, 2008, 83: 67006
- 6 Rotter M, Tegel M, Johrendt D. Superconductivity at 38 K in the iron arsenide  $(\text{Ba}_{1-x}\text{K}_x)\text{Fe}_2\text{As}_2$ . *Phys Rev Lett*, 2008, 101: 107006
- 7 Chen G F, Li Z, Li G, et al. Superconductivity in hole-doped  $(\text{Sr}_{1-x}\text{K}_x)\text{Fe}_2\text{As}_2$ . *Chin Phys Lett*, 2008, 25: 3403–3405
- 8 Tapp J H, Tang Z, Lv B, et al.  $\text{LiFeAs}$ : An intrinsic  $\text{FeAs}$ -based superconductor with  $T_c=18$  K. *Phys Rev B*, 2008, 78: 66505
- 9 Hsu F C, Luo J Y, Yeh K W, et al. Superconductivity in the PbO-type structure  $\alpha\text{-FeSe}$ . *Proc Natl Acad Sci USA*, 2008, 105: 14262
- 10 Dong J, Zhang H, Xu J G, et al. Competing orders and spin-density-wave instability in  $\text{La}(\text{O}_{1-x}\text{F}_x)\text{FeAs}$ . *Europhys Lett*, 2008, 83: 27006
- 11 de la Cruz C, Huang Q, Lynn J W, et al. Magnetic order close to superconductivity in the iron-based Layered  $\text{La}(\text{O}_{1-x}\text{F}_x)\text{FeAs}$  systems. *Nature*, 2008, 453: 899–902
- 12 Lumsden M D, Christianson A D, Parshall D, et al. Two-dimensional resonant magnetic excitation in  $\text{BaFe}_{1.84}\text{Co}_{0.16}\text{As}_2$ . *Phys Rev Lett*, 2009, 102: 107005
- 13 Todorov I, Chung D Y, Malliakas C D, et al.  $\text{CaFe}_4\text{As}_3$ : A metallic iron arsenide with anisotropic magnetic and charge-transport properties. *J Am Chem Soc*, 2009, 131: 5405–5407
- 14 SKim J, Blasius T D, Kim E G, et al. Superconductivity in undoped single crystals of  $\text{BaFe}_2\text{As}_2$ : Field and current dependence. *J Phys Condens Matter*, 2009, 21: 342201
- 15 Chen G F, Li Z, Dong J, et al. Transport and anisotropy in single-crystalline  $\text{SrFe}_2\text{As}_2$  and  $\text{A}_{0.6}\text{K}_{0.4}\text{Fe}_2\text{As}_2$  ( $\text{A}=\text{Sr}, \text{Ba}$ ) Superconductors. *Phys Rev B*, 2008, 78: 224512
- 16 Kanaya K, Abe S, Yoshida H, et al. Magnetic and structural properties of pseudo-binary compounds  $\text{CrAs}_{1-x}\text{P}_x$ . *J Alloys Compd*, 2004, 383: 189–194
- 17 Watanabe H, Kazama N, Yamaguchi Y, et al. Magnetic structure of  $\text{CrAs}$  and Mn-substituted  $\text{CrAs}$ . *J Appl Phys*, 1969, 40: 1128
- 18 Boller H, Kallel A. Crystallographic distortion in  $\text{CrAs}_{0.50}\text{Sb}_{0.50}$ . *Solid State Commun*, 1973, 12: 665–671
- 19 Selte K, Kjekshus A, Jamison W, et al. Magnetic structural and properties of  $\text{CrAs}$ . *Acta Chem Scandinav*, 1971, 25: 1703–1714
- 20 Zhang G M, Su Y H, Lu Z Y, et al. Universal linear-temperature dependence of static magnetic susceptibility in iron-pnictides. *Europhys Lett*, 2009, 86: 37006
- 21 Wu G, Liu R H, Wang X F, et al. Different resistivity response to spin-density wave and superconductivity at 20 K in  $\text{Ca}_{1-x}\text{Na}_x\text{Fe}_2\text{As}_2$ . *J Phys Condens Matter*, 2008, 20: 422201
- 22 Huang Q, Qiu Y, Bao W, et al. Neutron-diffraction measurements of magnetic order and a structural transition in the parent  $\text{BaFe}_2\text{As}_2$  compound of  $\text{FeAs}$ -Based high-temperature superconductors. *Phys Rev Lett*, 2008, 101: 257003
- 23 Tsujii N, Yoshimura K, Kosuge K. Deviation from the Kadowaki-Woods relation in Yb-based intermediate-valence systems. *J Phys Condens Matter*, 2003, 15: 1993–2003
- 24 Zhao L L, Yi T H, Fettinger J C, et al. Fermi-liquid state and enhanced electron correlations in the iron pnictide  $\text{CaFe}_4\text{As}_3$ . *Phys Rev B*, 2009, 80: 020404
- 25 Foo M L, Wang Y, Watauchi S, et al. Charge ordering, commensurability, and metallicity in the phase diagram of the layered  $\text{Na}_x\text{CoO}_2$ . *Phys Rev Lett*, 2004, 92: 247001
- 26 Yan J Q, Kreyssig A, Nandi S, et al. Structural transition and anisotropic properties of single-crystalline  $\text{SrFe}_2\text{As}_2$ . *Phys Rev B*, 2008, 78: 024516
- 27 Wang X F, Wu T, Wu G, et al. Anisotropy in the electrical resistivity and susceptibility of superconducting  $\text{BaFe}_2\text{As}_2$  single crystals. *Phys Rev Lett*, 2009, 102: 117005